Biological Data 2026, 1(1), 44-54.
https://doi.org/????

Brief Reports

Exploratory Reanalysis of Substantia Nigra Transcriptomes in Parkinson's Disease

Amirhosein Akhoondi[1], Mostafa Rafiepour[1*], Farinaz Behfarjam[1*]

[1] Department of Genetics, Faculty of Science, Danesh Alborz University, Qazvin, Iran

***** Corresponding Authors: Mostafa Rafiepour & Farinaz Behfarjam
Email: mostafarafiepour@gmail.com & Behfarjam.farinaz@gmail.com

CITATION

Akhoondi, A., Rafiepour, M., & Behfarjam, F. (2026). Exploratory reanalysis of substantia nigra transcriptomes in Parkinson's disease. Biological Data, 1(1), 44–54. https://doi.org/xxxxxxxxx.

ARTICLE INFO

Received: March 10, 2026
Revised: April 24, 2026
Accepted: May 12, 2026
Available online: May 15, 2026

COPYRIGHT

© The author(s) retain the copyright.
Publisher: University of Kurdistan Press.
This is an open access article distributed under the terms of the Creative Commons Attribution-

Abstract: Small postmortem cohorts can yield plausible expression signals with unstable statistical significance. This short report reanalyzed deposited substantia nigra pars compacta counts from four Parkinson's disease (PD) donors and three controls (GSE206308). A condition-only PyDESeq2 model with Benjamini–Hochberg false discovery rate (FDR) control and fold-change shrinkage was complemented by leave-one-sample-out refits, limma-voom, direction-specific functional enrichment, and literature-defined marker scores. PyDESeq2 identified 406 genes at FDR < 0.05, including 125 higher and 281 lower in PD. Leave-one-out refits yielded 157–624 significant genes; only 109 of the primary 406 (26.8%) remained significant in every refit. limma-voom identified 11 significant genes, all contained in the primary and consistently retained sets, giving only 2.7% overlap with the primary list. Effect estimates nevertheless agreed closely across 17,888 genes (Spearman correlation 0.970). The lower-expression list was enriched for synaptic signaling, dopamine biosynthesis, and synaptic vesicle cycle; the higher-expression list included motor-protein annotations. A dopamine-marker transcript score was 3.23 log2 units lower in PD, but depletion relative to a pan-neuronal score was imprecise. This reanalysis illustrates substantial sample and method sensitivity despite coherent expression directions. Small sample size, demographic imbalance, and unresolved tissue composition limit biological attribution and motivate explicit stability reporting in future studies.

Keywords: RNA Sequencing, Differential Gene Expression, Sensitivity Analysis, Dopaminergic Neurons, Functional Enrichment

1. Introduction

Parkinson's disease (PD) is characterized by degeneration of dopaminergic neurons in the substantia nigra pars compacta (SNpc). Transcriptomic studies provide a means of examining associated molecular changes, but their interpretation depends on the sampled tissue, cellular composition, and clinical characteristics. Single-cell profiling has identified dopamine-neuron populations with different vulnerability to PD, emphasizing that changes in bulk tissue expression may reflect both altered cellular abundance and changes within surviving cells (Kamath et al., 2022). Several transcription factors involved in dopaminergic differentiation also maintain neuronal properties in adulthood. Experimental studies demonstrate continuing roles for FOXA1/FOXA2 in dopaminergic function and for LMX1A/LMX1B in mitochondrial integrity and neuronal survival (Doucet-Beaupré et al., 2016; Pristerà et al., 2015). Consequently, developmental annotations in adult tissue do not directly establish altered brain development. Verma et al. (2023) reported reduced expression of dopaminergic-identity and neurotransmission-related genes in human PD SNpc and deposited the corresponding RNA-seq data. Other PD transcriptomic studies have combined multiple cohorts, network analysis, and validation to prioritize candidate genes (Yao et al., 2025; Zhou et al., 2023). This short report reanalyzes the deposited human gene counts from Verma et al. (2023), using explicit multiple-testing control, fold-change shrinkage, and sensitivity analyses of sample inclusion and statistical method. Direction-specific enrichment and literature-defined marker scores provide functional and tissue-composition context. The contribution is a transparent illustration of how significance lists can vary in a small postmortem cohort, intended to help future researchers report stability alongside effect estimates.

2. Methods

2.1. Data Acquisition and Cohort Description

All seven human postmortem bulk SNpc libraries from GSE206308/SRP382117 were reanalyzed (four PD, three non-PD controls; Table 1). These paired-end HiSeq 2500 data originated from anatomically microdissected tissue, not isolated neurons (Verma et al., 2023). The complete GEO series and linked run inventory contain seven human and 16 separate mouse libraries. No human C3 or PD3 record is deposited under these accessions; the public metadata do not explain the nonconsecutive human labels. All deposited human libraries were retained, and mouse libraries were excluded by species. The deposited GRCh37/TopHat2/HTSeq integer counts were used; raw-read processing was not repeated. The published RNA-seq cohort comprised two female/two male PD donors aged 80–83 years and three male controls aged 69–85 years. Individual clinical cases could not be securely linked to library identifiers, preventing covariate adjustment. Upstream versions, repository inventories, group-level postmortem intervals, RNA integrity, and comorbidities are documented in Supplementary File 1.

Table 1. Human RNA-seq libraries included in the reanalysis.

Library	GEO accession	SRA accession	Group
C1	GSM6250333	SRR19697827	Non-PD control
C2	GSM6250334	SRR19697826	Non-PD control
C4	GSM6250335	SRR19697825	Non-PD control
PD1	GSM6250336	SRR19697824	PD
PD2	GSM6250337	SRR19697823	PD
PD4	GSM6250338	SRR19697822	PD
PD5	GSM6250339	SRR19697821	PD

Note: Nonconsecutive labels reproduce the public human deposit, not exclusions made in this reanalysis. No explanation for the absent human C3/PD3 labels is available in the public metadata. PD1 was omitted only in specified sensitivity analyses. Donor demographics are reported at cohort level because a verified donor-to-library crosswalk was unavailable.

2.2. Count Provenance and Quality Assessment

After removing five HTSeq summary counters, gene identifiers and nonnegative integer counts were checked for completeness and uniqueness. Depth, assigned counts, and detected genes were summarized (Table 2). Principal component analysis (PCA) used the 500 most variable genes after log2(normalized count + 1) transformation; all libraries were retained. Read-quality, duplication, and alignment metrics were not re-estimated.

2.3. Differential Gene Expression Analysis

PyDESeq2 0.5.2 (Python 3.12.14) was run with design ~ condition and explicit PD/control contrast (Muzellec et al., 2023; Love et al., 2014). Genes required ≥10 counts in ≥3 samples. Median-of-ratios normalization, parametric dispersion estimation, and negative-binomial Wald tests were used. Positive effects indicate higher expression in PD. This model was not adjusted for donor characteristics. Independent filtering used alpha=0.05; significance required Benjamini–Hochberg adjusted $p < 0.05$ (Benjamini & Hochberg, 1995). Package Cook's-distance filtering was enabled and count replacement disabled. Adaptive apeglm-based shrinkage was used for effect display, without changing Wald p values (Zhu et al., 2019). A secondary |shrunken log2FC| ≥ 1.5 subset was descriptive, not the enrichment input. Exact outlier rules, parameters, and complete outputs are in Supplementary File 1.

2.4. Sample and Method Sensitivity Analyses

The original six-library subset was reanalyzed with its expression filter reapplied. Seven additional leave-one-out refits retained the primary gene universe and repeated inference to assess direction and significance stability. These internal sensitivity analyses do not provide independent validation; implementation details are in Supplementary File 1. A complementary limma-voom analysis used the same seven integer-count libraries and fixed 17,888-gene expression-filtered universe (Ritchie et al., 2015; Law et al., 2014). R 4.5.3, edgeR 4.10.6, and limma 3.68.5 were used with TMM normalization of retained-gene library totals and a condition-only PD/control coefficient. edgeR: voomLmFit fitted observation-weighted linear models with zero-count degrees-of-freedom correction (Chen et al., 2025; Lun & Smyth, 2017). LOWESS span was fixed at 0.5; adaptive span and sample-quality weights were disabled. Robust empirical-Bayes moderation used robust=TRUE and trend=FALSE (Phipson et al., 2016). BH adjustment covered all finite limma-voom tests, with adjusted $p < 0.05$ and no fold-change cutoff. PyDESeq2 Cook and independent filters were not imposed on limma-voom. One complementary configuration was specified before fitting; no alternative settings were selected after

inspecting its results. Effect agreement compares unshrunken coefficients. This same-data comparison is not independent validation.

2.5. Direction-Specific Functional Enrichment

Gene Ontology Biological Process, Molecular Function, and Cellular Component (GO BP/MF/CC) and Kyoto Encyclopedia of Genes and Genomes (KEGG) over-representation were evaluated with the 17,130 finite-adjusted-p genes as the custom background (Kolberg et al., 2023). The combined 406-gene query was retained for comparison and split into the 125 positive and 281 negative primary maximum-likelihood coefficients, without a magnitude cutoff. Frozen g:Profiler mappings and complete term-by-gene memberships were used to recompute one-sided hypergeometric tests offline. BH $q < 0.05$ was applied separately within each source and direction over terms with nonzero query overlap. All evidence types were retained; unmapped identifiers were excluded. The frozen service version was e114_eg62_p19_27110d83 (October 11, 2026; Ensembl 114; GO January 23, 2026; KEGG March 15, 2026). All 6,277 original overlapping terms had complete query evidence vectors, allowing exact directional subset reconstruction. Recalculation reproduced every combined-query q value within 3.7×10^{-15}. Sensitivity outputs additionally fix each source's original combined-term family, assign p=1 to directional zero overlaps, and pool tests across directions or sources. These families can change borderline decisions. Gene-list direction does not establish pathway activation or inhibition. Full specifications, contributing genes, and all corrections are supplied in Supplementary File 1. No protein–protein interaction (PPI) or centrality analysis was performed.

2.6. Marker Scores and Tissue Composition

A literature-defined dopamine-marker score used TH, SLC6A3, and SLC18A2 (Kamath et al., 2022). Disjoint pan-neuronal markers SYT1/SNAP25 and contextual astrocyte, oligodendrocyte, and microglial panels followed Martirosyan et al. (2024). The panels were fixed before computing this descriptive sensitivity check; several dopamine-marker decreases were already known from the source study. Each library score was the equal-weight mean log2(primary-model size-factor-normalized count + 1). We calculated PD-minus-control differences, approximate Welch 95% confidence intervals, a dopamine-minus-pan-neuronal score contrast, and marker/library omission summaries. For the dopamine score, all 35 group-label assignments were enumerated for an exploratory two-sided equal-tailed benchmark. Its granularity and exchangeability assumptions differ from those of the Welch interval. Scores were not used as DE covariates or to estimate cell fractions or a composition-attributable percentage. Complete panels and calculations are in Supplementary File 1.

3. Results

3.1. Quality Assessment and Sample Structure

All seven count files passed structural checks. Archived read pairs ranged from 21.25 to 25.87 million and gene-assigned counts from 16.67 to 20.21 million per library (Table 2). Detected genes ranged from 25,187 to 28,602. These summaries describe sequencing depth and count availability; they do not establish the absence of technical bias. PCA explained 32.4% and 26.4% of variance on the first two components, respectively, and showed appreciable heterogeneity within the PD group (Supplementary Figure S1). PD5 separated from other libraries on the second component and was retained, with its influence assessed through sensitivity analysis.

Table 2. Sequencing-depth and count-level quality summaries.

Library	Number of read pairs	Gene-assigned counts	Detected genes	Size factor
C1	24,630,899	18,900,611	28,219	1.208
C2	21,246,728	16,881,260	25,187	0.831
C4	24,506,375	19,172,123	28,602	0.896
PD1	25,475,987	19,521,770	28,473	1.150
PD2	25,772,564	18,991,689	27,044	1.006
PD4	25,870,827	20,206,755	26,752	1.041
PD5	21,384,258	16,667,371	27,033	0.942

Note: Read-pair counts are SRA spots, not read length or individual-read counts. Detected genes have at least one count. Gene-assigned counts are from deposited HTSeq files; size factors are from the primary PyDESeq2 model. Neither assigned-count fractions nor size factors are STAR mapping rates.

3.2. Differential Gene Expression

Of 63,677 gene rows, 17,888 met the expression filter. Cook's-distance filtering withheld p values for 64 genes; a further 694 genes had finite raw p values but were excluded by independent filtering, leaving 17,130 genes with adjusted p values. In the primary condition-only model, 406 genes met FDR < 0.05: 125 had positive and 281 negative PD-versus-control estimates (Supplementary Figure S2). Of these, 125 also met |shrunken log2 fold change| ≥ 1.5 (19 higher and 106 lower in PD). These are model- and threshold-dependent counts, not a validated inventory of PD-specific genes. Selected genes implicated in dopaminergic biology showed negative PD-versus-control estimates (Table 3). For example, shrunken log2 fold changes were −3.84 for SLC6A3, −3.23 for SLC18A2, −2.36 for TH, and −3.09 for LMX1B. Individual normalized counts illustrate between-sample variability (Supplementary Figure S3). Table 3 retains the illustrative primary estimates and adds limma-voom adjusted p values; these genes were not selected by network centrality or by agreement between methods.

Table 3. Selected primary gene associations and complementary method results.

Gene	Shrunken log2FC	MLE log2FC (95% CI)	PyDESeq2 BH p	limma-voom BH p
AGTR1	-3.95	-4.07 (-5.00, -3.13)	3.95e-14	0.0362
DDC	-3.46	-3.57 (-4.41, -2.73)	1.19e-13	0.0580
EN1	-2.17	-2.30 (-3.03, -1.56)	5.23e-07	0.1184
FOXA2	-2.36	-2.72 (-4.01, -1.43)	0.0042	0.1780
LMX1B	-3.09	-3.31 (-4.46, -2.17)	6.56e-06	0.1780
NR4A2	-1.51	-1.74 (-2.56, -0.91)	0.0041	0.1910
NTSR1	-3.64	-3.78 (-4.75, -2.81)	2.74e-11	0.1011
PITX3	-2.51	-2.82 (-4.07, -1.58)	0.0013	0.1778
SLC18A2	-3.23	-3.30 (-3.96, -2.64)	8.54e-19	0.0211
SLC6A3	-3.84	-3.95 (-4.83, -3.06)	1.02e-14	0.0414
TH	-2.36	-2.58 (-3.57, -1.58)	1.00e-04	0.1612

Note: All contrasts are PD/control. The shrunken and maximum-likelihood estimates (MLE) and approximate unadjusted Wald intervals are from PyDESeq2; intervals are MLE ± 1.96 × standard error and do not describe the shrunken estimates. BH p denotes method-specific adjusted p, using each method's reported testing family. The gene selection is illustrative; the complete 17,888-gene comparison and all 11 shared discoveries are in Supplementary File 1.

3.3. Sample and Method Sensitivity

The separately filtered six-library analysis identified 306 genes at FDR < 0.05, of which 234 overlapped the primary set. Fixed-universe leave-one-sample-out refits yielded 157–624 significant genes and retained 129–325 of the primary 406 in an individual refit (Figure 1A). Only 109 of 406 (26.8%) remained significant in all seven refits, although all 406 retained the same estimated direction. Excluding PD1 yielded 303 genes with the fixed primary universe, compared with 306 when the six-library expression filter was reapplied. These differences demonstrate sensitivity to both sample inclusion and filtering. limma-voom produced 17,888 finite adjusted p values and identified only 11 genes at BH-adjusted p < 0.05, all lower in PD. All 11 belonged to both the 406 primary genes and the 109 genes significant in every PyDESeq2 leave-one-out refit. Thus, 11/406 primary genes (2.7%; Jaccard index 0.027) were significant in both methods, leaving 395 PyDESeq2-only and no limma-voom-only discoveries. Nevertheless, effect directions agreed for all 406 primary genes and for 17,056/17,888 genes overall (95.3%). Unshrunken log2 fold changes correlated strongly across all genes (Spearman ρ = 0.970; Figure 1B). This marked discrepancy in significance lists, despite similar effects, indicates substantial dependence on the statistical procedure; it does not validate the primary gene list.

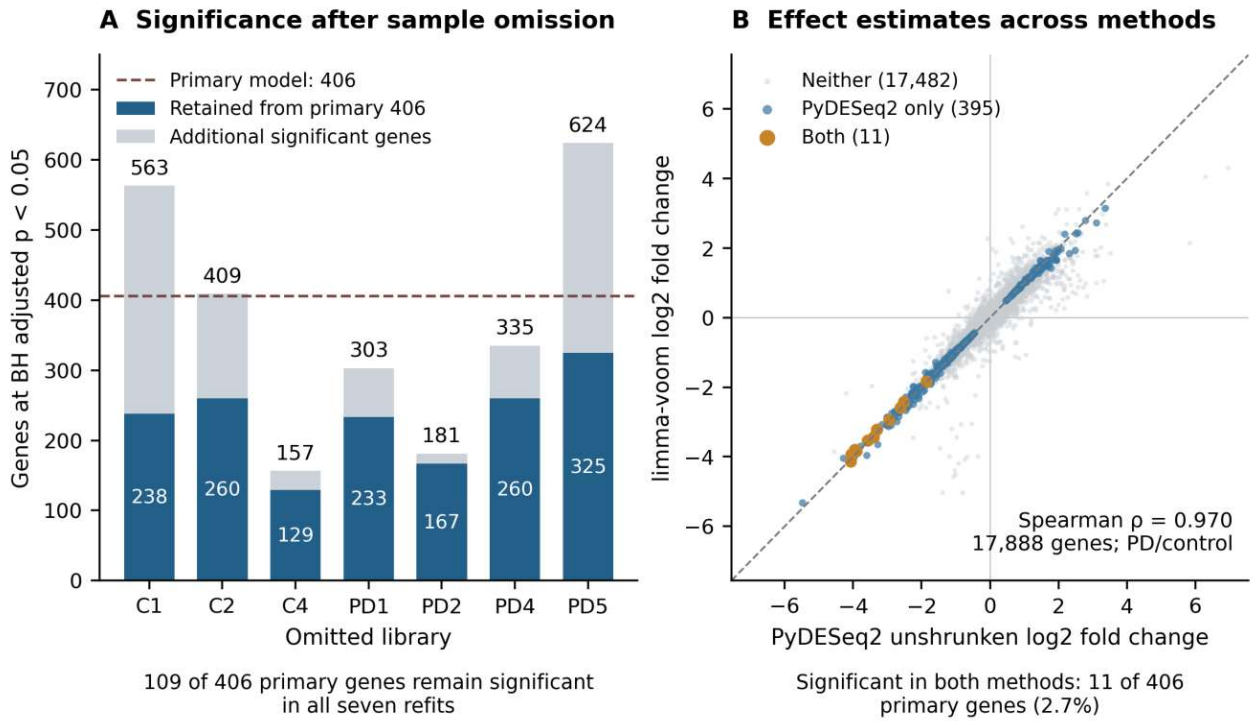


Figure 1. Sample and method sensitivity of differential expression.
(A) Total BH-significant genes after omitting each library; blue segments show retained members of the primary 406-gene list, and gray segments show additional genes. The dashed line marks the primary total. Only 109 primary genes are significant in every refit.
(B) Unshrunken PD/control coefficients from PyDESeq2 and limma-voom for all 17,888 expression-filtered genes. Colors indicate method-specific significance: neither method, PyDESeq2 only, or both. Only 11 genes meet BH-adjusted p < 0.05 in both methods. The diagonal indicates equal coefficients; agreement of effects is distinct from agreement of significance.

3.4. Direction-Specific Enrichment

The combined query mapped 393/406 genes and 16,577/17,130 background genes. It retained the previously reported 176 BP, two MF, 78 CC, and four KEGG associations. Splitting by coefficient sign mapped 124/125 higher-expression and 269/281 lower-expression genes. The lower list yielded 218 BP, 17 MF, 80 CC, and seven KEGG associations; the higher list yielded no BP, 15 MF, five CC, and one KEGG association (Table 4). These counts represent overlapping annotations, not independent mechanisms.

Table 4. Enrichment counts for combined and direction-specific queries.

Query	Input/mapped genes	GO BP	GO MF	GO CC	KEGG
Combined	406 / 393	176 / 4,332	2 / 1,046	78 / 628	4 / 271
Higher in PD	125 / 124	0 / 2,065	15 / 490	5 / 334	1 / 134
Lower in PD	281 / 269	218 / 3,777	17 / 881	80 / 527	7 / 236

Note: GO/KEGG cells show significant/overlapping terms tested. BH correction is separate within each source and query, with $q < 0.05$. The background contains 16,577 mapped genes. Both combined-query MF terms are marginal at $q = 0.0471$. Fixed-family and pooled-direction corrections and complete term-level results are supplied in Supplementary File 1.

The lower-expression list contained all six combined-query dopamine-biosynthesis hits and all 12 synaptic-vesicle-cycle hits. Lower-list q values were 2.17×10^{-14} for synaptic signaling, 4.84×10^{-6} for dopamine biosynthesis, and 1.39×10^{-7} for synaptic vesicle cycle. The higher list included cytoskeletal motor activity (six hits; q=0.0105) and Motor proteins (seven hits; q=0.0139). These associations remained significant under the exported correction sensitivities. Neuroactive ligand–receptor interaction, significant in the combined query, did not meet $q < 0.05$ in either direction (Table 5).

Table 5. Selected KEGG results across combined and directional queries.

KEGG pathway	Combined q	Higher-in-PD q	Lower-in-PD q
Synaptic vesicle Cycle hsa04721	1.12e-05	— (0 hits)	1.39e-07
Neuroactive ligand-receptor Interaction hsa04080	0.0174	0.3332	0.0601
Motor proteins hsa04814	0.2494	0.0139	0.9258

Note: This is a selected display. The dash indicates zero higher-list overlap; no q value is assigned in that query's primary nonzero-overlap family, while fixed-family sensitivities assign p=1. The four combined-query KEGG results, all eight directional significant results, and contributing genes are retained in Supplementary File 1. Gene-list direction and pathway labels do not measure pathway activation or inhibition.

The two combined-query MF terms (q=0.0471) and two combined-query KEGG terms ($q \approx 0.0495$) are marginal. The latter labels and their gene memberships are retained in the supplement as shared-annotation overlaps rather than biological interpretations. Directional splitting also exposes family-sensitive MF decisions: lower-list cation-transporter activity changes from q=0.0429 to 0.0509 under the fixed source family, while calcium-channel-inhibitor activity changes from q=0.0398 to 0.0631 when both directions are pooled within MF. Such near-threshold associations are not emphasized as firm mechanisms.

3.5. Marker Scores and Tissue Composition

The literature-defined dopamine-marker score was lower in PD by 3.23 log2 score units (PD-minus-control difference −3.23; approximate Welch 95% CI −4.82 to −1.63; Figure 2A). The coarse two-sided equal-tailed benchmark over all 35 label assignments was p=0.0571. The pan-neuronal score was also lower on average (−1.89; 95% CI −3.78 to 0.01). The dopamine-minus-pan-neuronal difference was −1.34 (95% CI −3.63 to 0.95; Figure 2B), leaving substantial uncertainty about relative depletion beyond broader neuronal transcript signal. Omitting individual dopamine markers retained negative score contrasts (−3.55 to −2.92); omitting individual libraries while retaining the primary size factors gave −3.64 to −2.85. Complete per-library scores, individual markers, and contextual glial panels are provided in Supplementary File 1 and Supplementary Figures S4–S5. These expression-derived checks are compatible with altered dopaminergic cellular contribution, but cannot distinguish cell loss from within-cell transcriptional changes or quantify the proportion of DE attributable to composition.

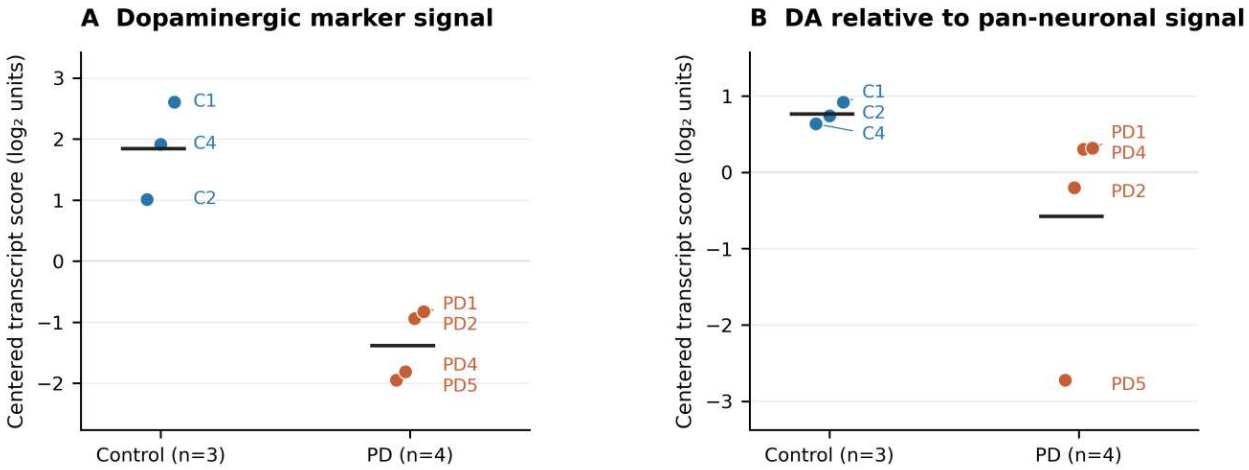


Figure 2. Cell-type marker transcript scores across the seven human SNpc libraries. (A) Dopamine (DA) marker score: mean log2(normalized count + 1) for TH, SLC6A3, and SLC18A2. (B) Dopamine score minus the mean score for the disjoint pan-neuronal markers SYT1 and SNAP25. Scores are centered across all seven libraries for display. Each point represents one library; labels correspond to Table 1, and black lines show group means. These bulk transcript scores are not cell fractions, and panel B is not a dopamine-neuron proportion.

4. Discussion

The principal contribution of this short reanalysis is the separation of effect-direction agreement from significance-list stability. Only 109/406 primary genes remained significant in every sample-omission refit, and only 11/406 were significant with limma-voom, despite strong coefficient agreement. The discrepancy reflects sensitivity to modeling, variance estimation, normalization, and method-specific testing families; this dataset cannot identify a single explanation or determine which method's discoveries are biologically true. Reporting the full effect estimates, selection frequencies, and method comparison makes the uncertainty visible and provides a useful template for future small-cohort studies. Interpretation of the expression associations requires consideration of the established molecular identity of dopaminergic neurons. Genes emphasized in the source study, including TH, DDC, SLC6A3, and SLC18A2, participate in dopamine synthesis or transport and are therefore biologically plausible findings in SNpc tissue (Verma et al., 2023). Related transcriptomic work has also prioritized DDC and SLC18A2 (Yao et al., 2025). Their recurrence provides biological

context but does not establish novel regulatory functions, diagnostic performance, or therapeutic efficacy. Because the present analysis reuses the deposited cohort, agreement with Verma et al. (2023) represents consistency within the same underlying observations, not independent replication. The marker-score analysis quantifies a depleted dopamine-related transcript signal but does not provide a cell-count estimate. The pan-neuronal decrease and imprecise dopamine-minus-pan-neuronal contrast are compatible with tissue-composition effects, without establishing their magnitude. Marker expression can change in surviving cells, and vulnerable dopamine-neuron subtypes differ in abundance and molecular identity (Kamath et al., 2022). The literature-defined panels are descriptive checks on the same expression data, not deconvolution or independent confirmation. Accordingly, no percentage of the differential-expression signal is assigned to neuronal loss. Direction-specific enrichment locates the principal synaptic and dopamine-related annotation overlaps in the lower-expression list. The higher-list motor-protein annotations likewise describe gene membership, not motor behavior or pathway activation. Development-related GO annotations provide functional context because genes characterized during development can remain active in mature neurons (The Gene Ontology Consortium, 2019). Adult-mouse experiments support continuing FOXA1/FOXA2 and LMX1A/LMX1B functions (Doucet-Beaupré et al., 2016; Pristerà et al., 2015). Neither these overlaps nor differential expression establish developmental mechanisms or network centrality. PPI-based findings in other studies remain distinct from this count-level reanalysis (Yao et al., 2025; Zhou et al., 2023).

4.1. Limitations

Only four PD and three control libraries are available, limiting power, variance estimation, and the stability of gene selection; FDR control and shrinkage cannot compensate for limited replication (Love et al., 2014; Schurch et al., 2016; Zhu et al., 2019). The PD cohort includes two female and two male donors, whereas all controls are male; sex can influence nigral expression (Cantuti-Castelvetri et al., 2007). Age ranges overlap, but age distributions and postmortem intervals differ. The unavailable donor-to-library crosswalk prevents justified adjustment for these characteristics, and RNA integrity, medication, comorbidities, and other donor factors remain uncontrolled. Marker scores cannot separate neuronal abundance from cell-state changes, estimate composition-attributable fractions, or remove confounding. The Welch intervals and label-enumeration benchmark rely on different small-sample assumptions and are exploratory. Reuse of deposited GRCh37 counts limits raw-read and alignment reassessment. Enrichment depends on the query, background, annotation, and correction family, with several marginal associations. Finally, sample-omission refits and the second method reuse one observational cohort; no independent cohort, PPI-network analysis, or experimental validation is available.

5. Conclusion and Future Work

This short report illustrates how apparently coherent expression differences can produce unstable significance lists in a small postmortem cohort. The 406-gene primary list contracts to 109 genes consistently significant across sample omissions and 11 genes shared with limma-voom. Lower dopamine-related transcript scores and direction-specific synaptic enrichment provide biological context, while unresolved composition and donor effects constrain attribution. Future studies should report sample and method sensitivity, use larger balanced cohorts with linked donor metadata, and incorporate cell-type-resolved validation. Reprocessing the raw reads with a current pipeline, a documented GRCh38 annotation, and renewed quality control would strengthen the technical basis of the analysis, although it would not correct the cohort's sampling limitations.

Data and Code Availability: Raw sequencing data are available under SRP382117 and deposited gene-count files under GSE206308. Supplementary File 1 (Supplementary_Analysis.zip) provides the unchanged seven human count inputs, accession and provenance records, executable scripts and dependency versions, full PyDESeq2 and leave-one-out outputs, limma-voom results and diagnostics, frozen combined and directional enrichment specifications and results, marker-score calculations, and supplementary figures. File checksums and reproduction instructions are included. The donor-to-library clinical crosswalk is not available.

Conflicts of Interest: The authors declare no conflict of interest.
AI Use and Originality Declaration: Generative AI was used to assist with manuscript editing and development of analysis scripts. The authors retain responsibility for verifying the analyses and for the accuracy, originality, integrity, and final content of this work.

References

Benjamini, Y., & Hochberg, Y. (1995). Controlling the false discovery rate: A practical and powerful approach to multiple testing. *Journal of the Royal Statistical Society: Series B (Methodological),* 57(1), 289-300. https://doi.org/10.1111/j.2517-6161.1995.tb02031.x

Cantuti-Castelvetri, I., Keller-McGandy, C., Bouzou, B., Asteris, G., Clark, T.W., Frosch, M.P., & Standaert, D.G. (2007). Effects of gender on nigral gene expression and Parkinson disease. *Neurobiology of Disease,* 26(3), 606-614. https://doi.org/10.1016/j.nbd.2007.02.009

Chen, Y., Chen, L., Lun, A.T.L., Baldoni, P.L., & Smyth, G.K. (2025). edgeR v4: Powerful differential analysis of sequencing data with expanded functionality and improved support for small counts and larger datasets. *Nucleic Acids Research,* 53(2), Article gkaf018. https://doi.org/10.1093/nar/gkaf018

Doucet-Beaupré, H., Gilbert, C., Profes, M.S., Chabrat, A., Pacelli, C., Giguère, N., Rioux, V., Charest, J., Deng, Q., Laguna, A., Ericson, J., Perlmann, T., Ang, S.L., Cicchetti, F., Parent, M., Trudeau, L.E., & Lévesque, M. (2016). Lmx1a and Lmx1b regulate mitochondrial functions and survival of adult midbrain dopaminergic neurons. *Proceedings of the National Academy of Sciences of the United States of America,* 113(30), E4387-E4396. https://doi.org/10.1073/pnas.1520387113

Kamath, T., Abdulraouf, A., Burris, S.J., Langlieb, J., Gazestani, V., Nadaf, N.M., Balderrama, K., Vanderburg, C., & Macosko, E.Z. (2022). Single-cell genomic profiling of human dopamine neurons identifies a population that selectively degenerates in Parkinson's disease. *Nature Neuroscience,* 25(5), 588-595. https://doi.org/10.1038/s41593-022-01061-1

Kolberg, L., Raudvere, U., Kuzmin, I., Adler, P., Vilo, J., & Peterson, H. (2023). g: Profiler—Interoperable web service for functional enrichment analysis and gene identifier mapping (2023 update). *Nucleic Acids Research,* 51(W1), W207-W212. https://doi.org/10.1093/nar/gkad347

Law, C.W., Chen, Y., Shi, W., & Smyth, G.K. (2014). voom: Precision weights unlock linear model analysis tools for RNA-seq read counts. *Genome Biology,* 15(2), R29. https://doi.org/10.1186/gb-2014-15-2-r29

Love, M.I., Huber, W., & Anders, S. (2014). Moderated estimation of fold change and dispersion for RNA-seq data with DESeq2. *Genome Biology,* 15, 550. https://doi.org/10.1186/s13059-014-0550-8

Lun, A.T.L., & Smyth, G.K. (2017). No counts, no variance: Allowing for loss of degrees of freedom when assessing biological variability from RNA-seq data. *Statistical Applications in Genetics and Molecular Biology,* 16(2), 83-93. https://doi.org/10.1515/sagmb-2017-0010

Martirosyan, A., Ansari, R., Pestana, F., Hebestreit, K., Gasparyan, H., Aleksanyan, R., Hnatova, S., Poovathingal, S., Marneffe, C., Thal, D.R., Kottick, A., Hanson-Smith, V.J., Guelfi, S., Plumbly, W.,

Belgard, T. G., Metzakopian, E., & Holt, M.G. (2024). Unravelling cell type-specific responses to Parkinson's disease at single cell resolution. *Molecular Neurodegeneration,* 19, 7. https://doi.org/10.1186/s13024-023-00699-0

Muzellec, B., Teleńczuk, M., Cabeli, V., & Andreux, M. (2023). PyDESeq2: A Python package for bulk RNA-seq differential expression analysis. *Bioinformatics,* 39(9), btad547. https://doi.org/10.1093/bioinformatics/btad547

Phipson, B., Lee, S., Majewski, I.J., Alexander, W.S., & Smyth, G.K. (2016). Robust hyperparameter estimation protects against hypervariable genes and improves power to detect differential expression. *The Annals of Applied Statistics,* 10(2), 946-963. https://doi.org/10.1214/16-AOAS920

Pristerà, A., Lin, W., Kaufmann, A.K., Brimblecombe, K.R., Threlfell, S., Dodson, P.D., Magill, P.J., Fernandes, C., Cragg, S.J., & Ang, S.L. (2015). Transcription factors FOXA1 and FOXA2 maintain dopaminergic neuronal properties and control feeding behavior in adult mice. *Proceedings of the National Academy of Sciences of the United States of America,* 112(35), E4929-E4938. https://doi.org/10.1073/pnas.1503911112

Ritchie, M.E., Phipson, B., Wu, D., Hu, Y., Law, C.W., Shi, W., & Smyth, G.K. (2015). limma powers differential expression analyses for RNA-sequencing and microarray studies. *Nucleic Acids Research,* 43(7), e47. https://doi.org/10.1093/nar/gkv007

Schurch, N.J., Schofield, P., Gierliński, M., Cole, C., Sherstnev, A., Singh, V., Wrobel, N., Gharbi, K., Simpson, G.G., Owen-Hughes, T., Blaxter, M., & Barton, G.J. (2016). How many biological replicates are needed in an RNA-seq experiment and which differential expression tool should you use? *RNA,* 22(6), 839-851. https://doi.org/10.1261/rna.053959.115

The Gene Ontology Consortium. (2019). The Gene ontology resource: 20 years and still GOing strong. *Nucleic Acids Research,* 47(D1), D330-D338. https://doi.org/10.1093/nar/gky1055

Verma, A., Kommaddi, R.P., Gnanabharathi, B., Hirsch, E.C., & Ravindranath, V. (2023). Genes critical for development and differentiation of dopaminergic neurons are downregulated in Parkinson's disease. *Journal of Neural Transmission,* 130(4), 495-512. https://doi.org/10.1007/s00702-023-02604-x

Yao, X., Wang, P., Huang, Z., & Li, L. (2025). Differential gene expression and immune profiling in Parkinson's disease: Unveiling potential candidate biomarkers. *BMC Neurology,* 25, 354. https://doi.org/10.1186/s12883-025-04388-x

Zhou, Y., Li, Z., Chi, C., Li, C., Yang, M., & Liu, B. (2023). Identification of hub genes and potential molecular pathogenesis in substantia nigra in Parkinson's disease via bioinformatics analysis. *Parkinson's Disease,* 2023, 6755569. https://doi.org/10.1155/2023/6755569

Zhu, A., Ibrahim, J.G., & Love, M.I. (2019). Heavy-tailed prior distributions for sequence count data: Removing the noise and preserving large differences. *Bioinformatics,* 35(12), 2084-2092. https://doi.org/10.1093/bioinformatics/bty895